Systems/Circuits

Norepinephrine Activates Dopamine D_4 Receptors in the Rat Lateral Habenula

David H. Root,[1]* Alexander F. Hoffman,[2]* Cameron H. Good,[2] Shiliang Zhang,[1] Eduardo Gigante,[1] Carl R. Lupica,[2]† and Marisela Morales[1]†

[1]Neuronal Networks Section, Integrative Neuroscience Research Branch and [2]Electrophysiology Research Section, Cellular Neurobiology Research Branch, National Institute on Drug Abuse, Baltimore, Maryland 21224

The lateral habenula (LHb) is involved in reward and aversion and is reciprocally connected with dopamine (DA)-containing brain regions, including the ventral tegmental area (VTA). We used a multidisciplinary approach to examine the properties of DA afferents to the LHb in the rat. We find that >90% of VTA tyrosine hydroxylase (TH) neurons projecting to the LHb lack vesicular monoamine transporter 2 (VMAT2) mRNA, and there is little coexpression of TH and VMAT2 protein in this mesohabenular pathway. Consistent with this, electrical stimulation of LHb did not evoke DA-like signals, assessed with fast-scan cyclic voltammetry. However, electrophysiological currents that were inhibited by L741,742, a DA-D_4-receptor antagonist, were observed in LHb neurons when DA uptake or degradation was blocked. To prevent DA activation of D_4 receptors, we repeated this experiment in LHb slices from DA-depleted rats. However, this did not disrupt D_4 receptor activation initiated by the dopamine transporter inhibitor, GBR12935. As the LHb is also targeted by noradrenergic afferents, we examined whether GBR12935 activation of DA-D_4 receptors occurred in slices depleted of norepinephrine (NE). Unlike DA, NE depletion prevented the activation of DA-D_4 receptors. Moreover, direct application of NE elicited currents in LHb neurons that were blocked by L741,742, and GBR12935 was found to be a more effective blocker of NE uptake than the NE-selective transport inhibitor nisoxetine. These findings demonstrate that NE is released in the rat LHb under basal conditions and that it activates DA-D_4 receptors. Therefore, NE may be an important regulator of LHb function.

Key words: **addiction; depression; dopamine; habenula; locus ceruleus; ventral tegmental area**

Introduction

Dopamine (DA) neurons of the ventral tegmental area (VTA) are critical components of the brain reward circuitry (Wise and Rompre, 1989), and their potential regulation by the lateral habenula (LHb) has received substantial recent attention. This is because the LHb modulates DA neuron activity and is involved in processing reward and aversion (Matsumoto and Hikosaka et al., 2007; Bromberg-Martin and Hikosaka, 2011; Hong et al., 2011). Specifically, LHb stimulation produces aversive responses in rodents, in part by inhibiting midbrain DA neurons via activation of the rostromedial tegmental nucleus (RMTg) (Christoph et al., 1986; Ji and Shepard, 2007; Jhou et al., 2009a,b; Balcita-Pedicino et al., 2011; Hong et al., 2011; Stamatakis and Stuber, 2012; Brown and Shepard, 2013), or through direct excitation of subpopulations of VTA neurons participating in aversion-related circuits (Omelchenko et al., 2009; Lammel et al., 2012). Therefore, the LHb has been strongly implicated in the regulation of DA neuron activity and disorders involving aversive processing, such as depression and addiction (Paris and Cunningham, 1994; Friedman et al., 2010; Li et al., 2011; Jhou et al., 2013; Nair et al., 2013).

In addition to the role of LHb on the regulation of VTA DA neurons, a DA projection from VTA has been proposed to provide feedback to the LHb (Gruber et al., 2007; Good et al., 2013; Jhou et al., 2013). This was originally proposed based on the finding that VTA DA neuron lesions significantly reduced LHb DA concentrations in tissue homogenates (Phillipson and Pycock, 1982) and because LHb receives tyrosine hydroxylase (TH)-expressing fibers from the VTA (Skagerberg et al., 1984). However, recent work shows that VTA neurons expressing TH are molecularly heterogeneous (Li et al., 2013). Some of the VTA TH neurons have the capability to synthesize DA, as they coexpress TH and L-aromatic amino decarboxylase but lack the capacity for accumulating DA in synaptic vesicles due to the absence of the vesicular monoamine transporter 2 (VMAT2) (Li et al., 2013), which is the only known CNS vesicular transporter of DA (Guillot and Miller, 2009). The DA release capacity of VTA

Received Oct. 24, 2013; revised Jan. 12, 2015; accepted Jan. 18, 2015.

Author contributions: D.H.R., A.F.H., C.H.G., S.Z., E.G., C.R.L., and M.M. designed research; D.H.R., A.F.H., C.H.G., S.Z., and E.G. performed research; D.H.R., A.F.H., C.H.G., S.Z., E.G., C.R.L., and M.M. analyzed data; D.H.R., A.F.H., C.R.L., and M.M. wrote the paper.

This work was supported by the National Institute on Drug Abuse Intramural Research Program. Viruses were packaged by the National Institute on Drug Abuse Optogenetic and Transgenic Technology Core.

The authors declare no competing financial interests.

*D.H.R. and A.F.H. contributed equally to this work.

†M.M. and C.R.L. contributed equally to this work as co-senior authors.

Correspondence should be addressed to either of the following: Dr. Carl R. Lupica, Electrophysiology Research Section, Cellular Neurobiology Branch, National Institute on Drug Abuse, 251 Bayview Blvd, Baltimore, MD 21224, E-mail: clupica@intra.nida.nih.gov; or Dr. Marisela Morales, Neuronal Networks Section, Integrative Neuroscience Research Branch, National Institute on Drug Abuse, 251 Bayview Blvd, Baltimore, MD 21224. E-mail: mmorales@intra.nida.nih.gov.

C.H. Good's present address: Altus Engineering, 2843 Churchville Road, Churchville, MD 21028.

DOI:10.1523/JNEUROSCI.4525-13.2015

 0270-6474/15/353460-10$15.00/0

TH neurons lacking VMAT2 and their participation in neuronal circuits are unknown. However, VTA TH-expressing/VMAT2-negative neurons are consistently found in the anteromedial VTA (Li et al., 2013), where the majority of LHb-projecting VTA neurons are found (Phillipson and Griffith, 1980; Swanson, 1982; Skagerberg et al., 1984; Gruber et al., 2007; Root et al., 2014a). These observations led us to hypothesize that TH-positive/VMAT2-negative VTA neurons target the LHb in the rat. To test this, and to determine whether DA release is detected in LHb in the absence of VMAT2, we used anatomical, molecular, electrophysiological, electrochemical, and chemical lesion approaches. Here, we report that, whereas DA is not released via electrical stimulation of the LHb, the activation of DA-D_4 receptors is observed when uptake or degradation is inhibited. Surprisingly, the activation of D_4 receptors under these conditions occurs via the actions of endogenous norepinephrine (NE) instead of DA.

Materials and Methods

All animal procedures were performed in accordance with National Institute of Health Guidelines and approved by the National Institute on Drug Abuse IRP Animal Care and Use Committee.

Retrograde tracer injections. Four male Sprague Dawley rats (400–450 g) were anesthetized with Equithesin (3.3 ml/kg, i.p). in physiological saline. The retrograde tracer Fluoro-Gold (FG; 1% in cacodylate buffer, pH 7.5) was iontophoretically delivered unilaterally into the LHb (coordinates in mm: −3.4 anteroposterior; 0.9 mediolateral; 5.4 ventral from skull) through a glass micropipette (inner tip diameter between 18 and 36 μm) using 1 μA current, 5 s pulses, at 10 s intervals for 15 min. The micropipette was left in place for an additional 10 min to prevent backflow of tracer up the injection track.

Anterograde tracer injections. Sprague Dawley rats ($n = 4$) were anesthetized with 1–5% isofluorane. An AAV5-CaMKIIα-ChR2-mCherry vector was injected into VTA (500 nl, 100 nl/min, −5.4 mm anteroposterior, −2.0 mm mediolateral at 10°, −8.0 mm dorsoventral from skull) using the UltraMicroPump with Micro 4 controller, 10 μl Nanofil syringes, and 35 gauge needles (WPI). Syringes were left in place for 10 min following injections to minimize diffusion.

Tissue preparation for anatomical studies. One week after FG injections, or 6 weeks after virus injection, rats were anesthetized with chloral hydrate (0.5 ml/kg) and perfused transcardially with 4% (w/v) PFA in 0.1 M phosphate buffer (PB), pH 7.3. Brains were left in 4% PFA for 2 h at 4°C and transferred to 18% sucrose in PB overnight. Brains were frozen in dry ice and stored at −80°C. FG-injected rat brains were coronally sectioned through VTA (16 μm) and LHb (30 μm) and stored in 30% polyethylene glycol, 30% sucrose at −80°C. AAV-injected rat brains were coronally sectioned through VTA and LHb (50 μm) with a vibratome (VT1000S, Leica) and stored as described for FG-injected rat brains.

Characterization of retrograde labeled cells by TH immunofluorescence, FG immunolabeling, and in situ *hybridization.* Midbrain coronal sections were incubated for 2 h at 30°C with rabbit anti-FG antibody (1:500; AB153; Millipore) and mouse monoclonal anti-TH antibody (1:500; MAB318; Millipore) in antibody buffer (DEPC-treated PB with 0.5% Triton X-100) supplemented with Rnasin (40 U/L stock; 5 μl/ml of buffer; Promega). Sections were rinsed three times for 5 min each with DEPC-treated PB and incubated in biotinylated goat anti-rabbit antibody (1:200; Vector Laboratories) and fluorescein-conjugated donkey anti-mouse antibody (1:50; Jackson ImmunoResearch) in DEPC-treated PB supplemented with Rnasin for 1 h at 30°C. Sections were rinsed, transferred to 4% PFA, and visualized by epifluorescence with a Nikon Eclipse E 800 microscope to identify FG- or TH-labeled neurons. Sections were rinsed, incubated for 10 min in PB containing 0.5% Triton X-100, rinsed, treated with 0.2N HCl for 10 min, rinsed, and then acetylated in 0.25% acetic anhydride in 0.1 M triethanolamine, pH 8.0, for 10 min. Sections were then rinsed and postfixed with 4% PFA for 10 min. Before hybridization and after a final rinse, sections were incubated in hybridization buffer for 2 h at 55°C (50% formamide, 10% dextran sulfate, 5× Denhardt's solution, 0.62 M NaCl, 50 mM DTT, 10 mM EDTA, 20 mM PIPES, pH 6.8, 0.2% SDS, 250 μg/ml salmon sperm DNA, 250 g/ml tRNA). Sections were hybridized for 16 h at 55°C in hybridization buffer containing [^{35}S]- and [^{33}P]-labeled singlestranded antisense of rat VMAT2 (nucleotides 1487–1980, accession #BF550727) probes at 10^7 cpm/ml. Sections were treated with 4 μg/ml RNase A at 37°C for 1 h and washed with 1× SSC, 50% formamide at 55°C for 1 h and with 0.1× SSC at 68°C for 1 h. After SSC wash, sections were rinsed with PB and incubated for 1 h at room temperature in avidin-biotinylated HRP (1:200, ABC kit; Vector Laboratories). Sections were rinsed, and the peroxidase reaction was developed with 0.05% DAB and 0.03% H_2O_2. Sections were mounted on coated slides, which were dipped in Ilford K.5 nuclear tract emulsion (Polysciences; 1:1 dilution in double distilled water) and exposed in the dark at 4°C for 4 weeks before development.

Data analysis of retrogradely labeled cellular subpopulations. Sections were viewed, analyzed, and photographed with bright-field or epiluminescence microscopy using a Nikon Eclipse E 800 microscope fitted with 4× and 20× objective lenses. Subdivisions of the midbrain DA system were traced based on criteria described previously (Li et al., 2013). Single- and double-labeled neurons were observed within each traced region at high power (20× objective lens) and marked electronically. Neurons included in the present study were counted when the stained cell was at least 5 μm in diameter. TH/VMAT2 double-labeled material was analyzed using epiluminescence to increase the contrast of silver grains. A cell was considered to express VMAT2 or VGluT2 mRNA when its soma contained concentric aggregates of silver particles above background level. FG/VMAT2 double-labeled material was analyzed by the following procedure by three independent scorers: (1) silver grains corresponding to VMAT2 expression were focused under epiluminescence microscopy; (2) the path of epiluminescence light was blocked without changing the focus; and (3) bright-field light was used to determine whether a brown neuron, expressing FG in focus, contained the aggregates of silver grains seen under epiluminescence. Pictures were adjusted to match contrast and brightness by using Adobe Photoshop (Adobe Systems).

Characterization of anterogradely labeled axons by mCherry, TH, and VMAT2 immunofluorescence. LHb sections from wild-type rats injected with AAV5-CaMKII-ChR2-mCherry in the VTA were incubated for 1 h in PB supplemented with 4% BSA and 0.3% Triton X-100. Sections were then incubated with a mixture of mouse anti-mCherry antibody (632543; Clontech Laboratories, 1:500), sheep anti-TH antibody (AB1542; EMD Millipore, 1:1000 dilution), and rabbit anti-VMAT2 antibody (H-V004; Phoenix Pharmaceuticals, 1:1000 dilution) overnight at 4°C. After rinsing in PB, sections were incubated in a mixture of fluorescent secondary antibodies raised in donkey, AlexaFluor-594 anti-mouse (715-585-151; Jackson ImmunoResearch Laboratories, 1:100), AlexaFluor-488 anti-rabbit (711-545-152; Jackson ImmunoResearch Laboratories, 1:100 dilution), and AlexaFluor-647 anti-sheep (713-605-147; Jackson ImmunoResearch Laboratories, 1:100). After rinsing, sections were mounted with Vectashield mounting medium (H1000; Vector Laboratories) on slides and air-dried. Fluorescent images were collected with the Olympus FV1000 Confocal System.

Brain slice preparation. Brain slices were prepared using a vibrating tissue slicer (Leica VT1000S) according to previously published protocols (Jhou et al., 2013). Coronal slices (280 μm) containing the nucleus accumbens or LHb were transferred to a holding chamber containing normal aCSF consisting of (mM) the following: 126 NaCl, 3.0 KCl, 1.5 $MgCl_2$, 2.4 $CaCl_2$, 1.2 NaH_2PO_4, 11.0 glucose, and 26 $NaHCO_3$, saturated with 95% O_2/5% CO_2, at 35°C for 20–25 min, and maintained at room temperature. A single brain slice was submerged in a low-volume (170 μl) recording chamber integrated into a fixed stage of an upright microscope, and continuously perfused with warm (30°C–32°C) aCSF at 2 ml/min using a peristaltic pump. The aCSF was warmed using an inline solution heater (TC-324B, Warner Instruments). Drugs were prepared as stock solutions in H_2O or DMSO and diluted in aCSF to the indicated concentrations. DMSO was used at final concentrations between 0.025% and 0.05% v/v.

Patch-clamp electrophysiology. Visualization of LHb neurons was performed with an upright microscope equipped for epifluorescence and differential interference contrast microscopy (Zeiss Axioskop). Recording electrodes (3–5 MΩ) were filled with (in mM) the following: 140

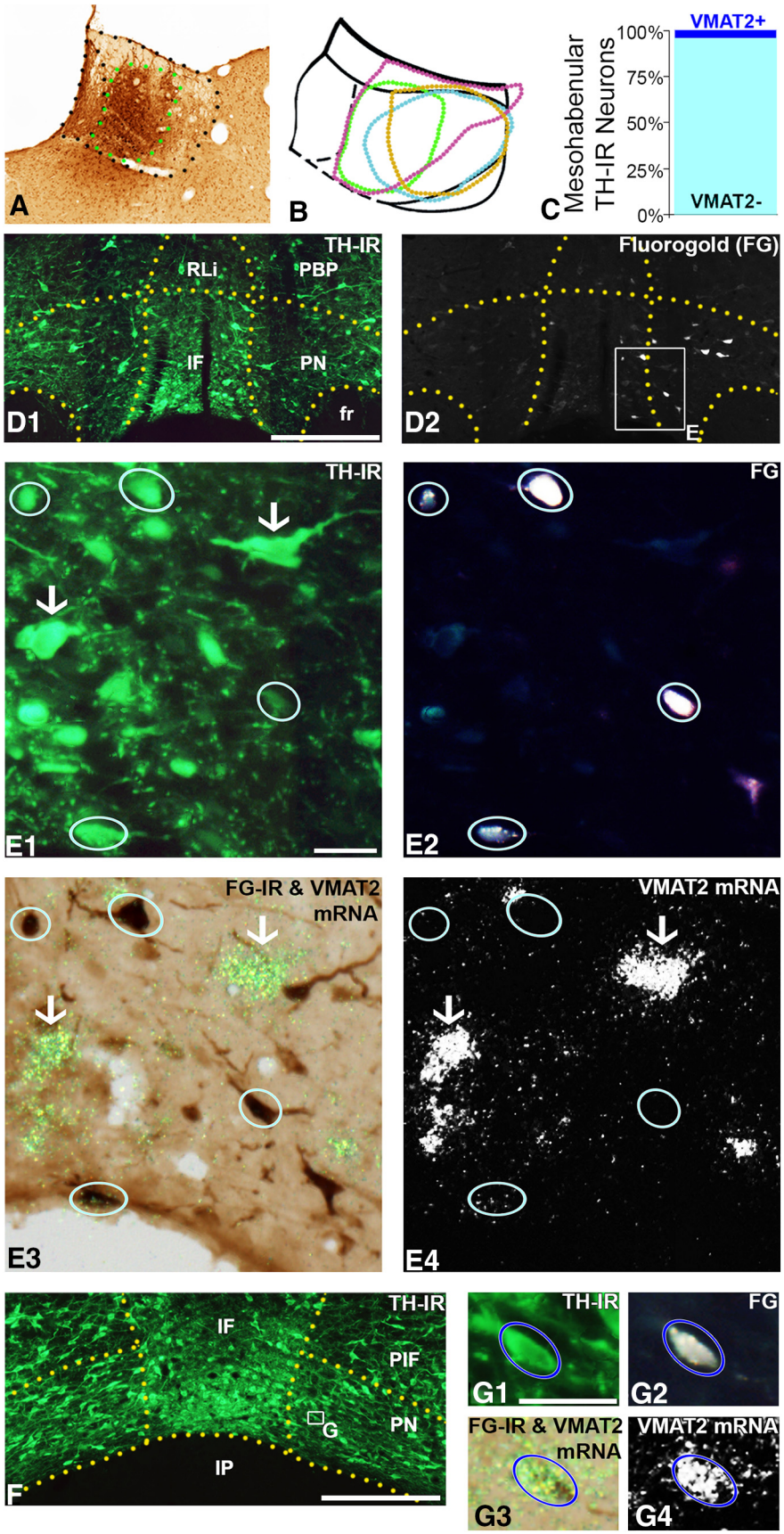

Figure 1. Mesohabenular TH neurons lack VMAT2 mRNA. ***A***, Detection of FG by immunoreactivity (IR) at the LHb injection site. ***B***, Each outline represents LHb FG injection sites within four different rats. LHb outline is modified from Paxinos and Watson (2007). ***C***, Mean percentage of mesohabenular TH-immunoreactive (TH-IR), neurons expressing or lacking VMAT2 mRNA (264 VMAT2-

K-gluconate, 5 KCl, 10 HEPES, 0.2 EGTA, 2 $MgCl_2$, 4 Mg-ATP, 0.3 Na_2-GTP, and 10 Na_2-phosphocreatine, pH 7.2 with KOH. Whole-cell voltage-clamp recordings were performed using an Axopatch 200B (Molecular Devices), WinLTP software (WinLTP), and an A/D board (National Instruments, PCI-6251) residing in a personal computer. Series resistance was monitored throughout recordings using brief hyperpolarizing steps (−10 mV, 200 ms). We excluded from analyses the cells that showed >10% change in series resistance. Unless otherwise indicated, cells were voltage-clamped at −60 mV.

Drug application to LHb slices. GBR12935 (Sigma-Aldrich), pargyline (Sigma-Aldrich), nisoxetine (Sigma-Aldrich), and L741,742 (Tocris Bioscience) were applied via bath superfusion. NE (Sigma-Aldrich) was delivered using a calibrated syringe pump (Razel Scientific Instruments). For pressure ejection experiments, NE (10 μM) was prepared in aCSF containing 2 μM ascorbic acid (Sigma-Aldrich) and applied via a micropipette (~5 μm tip opening) using a Picospritzer (General Valve).

Fast-scan cyclic voltammetry (FSCV). FSCV was performed using 7-μm-diameter carbon fiber (Goodfellow) electrodes. Pipettes containing the carbon fiber were filled with a solution of 4 M K-acetate/150 mM KCl and attached to the head stage of a patch-clamp amplifier (HEKA EVA-8, HEKA Instruments). Voltammetric scans, stimulus waveform generation and timing, and data collection were performed using A/D boards (PCI 6052E and PCI-6711E, National Instruments) and custom LabView-based software. All carbon fiber electrodes were tested for stable background currents and responsiveness in aCSF containing DA (2 μM) before, and following each experiment. Detection limits were calculated by multiplying the background noise (nA) by 3 and dividing by the calibration factor (nA/μM) for the electrode. Carbon fibers were placed at a depth of 75–100 μm within the tissue, either in the nucleus accumbens core or medial LHb. Voltammetric scans from −0.4 V to 1.3 V and from 1.3 V to −0.4 V were performed at 400 V/s at a frequency of 10 Hz. Single-pulse electrical stimulation (1–14 V, 1 ms) was performed using a bipolar stimulating electrode consisting of twisted formvar-insulated nickel-chrome wire (50 μm diameter). The input–output curve of the signals was similar to that observed using 10–300 μA constant current

←

from a total of 275 TH-IR neurons). ***D***, ***E***, TH-IR and FG-IR neurons within the VTA. ***E1–E4***, At higher magnification, circles represent mesohabenular neurons that contain both TH-IR (***E1***) and FG-IR (***E1***, ***E2***) but lack VMAT2 mRNA (***E3***, ***E4***). ***E1***, ***E3***, ***E4***, Arrows indicate examples of two TH-IR neurons expressing VMAT2 mRNA in the VTA but lacking FG. Scale bar: ***D1*** (applies also to ***D2***), 250 μm. Scale bar: ***E1*** (applies also to ***E1–E4***), 25 μm. ***F***, ***G***, Detection of TH-IR in the VTA. ***G1–G4***, Circles represent a mesohabenular neuron coexpressing TH-IR (***G1***), FG-IR (***G2***, ***G3***), and VMAT2 mRNA (***G3***, ***G4***). Scale bars: ***F***, 250 μm; ***G1*** (applies to ***G1–G4***), 25 μm.

Table 1. Subregional distribution of mesohabenular TH neurons[a]

	Rostral linear	Interfascicular	Paranigral	Parabrachial pigmented	Parainterfascicular	Rostral VTA
Rat 1	16.13%	29.03%	37.1%	9.68%	8.06%	0%
	($n = 10$)	($n = 18$)+	($n = 23$)	($n = 6$)++	($n = 5$)	($n = 0$)
Rat 2	30.65%	45.16%	11.29%	12.9%	0%	0%
	($n = 19$)	($n = 28$)++	($n = 7$)	($n = 8$)	($n = 0$)	($n = 0$)
Rat 3	11.94%	20.9%	31.34%	29.85%	4.48%	1.49%
	($n = 8$)	($n = 14$)	($n = 21$)+	($n = 20$)	($n = 3$)	($n = 1$)
Rat 4	7.14%	55.95%	30.95%	3.57%	2.38%	0%
	($n = 6$)	($n = 47$)++	($n = 26$)+	($n = 3$)+	($n = 2$)+	($n = 0$)

[a]Percent of retrogradely labeled neurons expressing TH protein within distinct VTA subnuclei. +, 1 VMAT2-expressing mesohabenular TH neuron; ++, 2 VMAT2-expressing mesohabenular TH neurons.

stimulation in previous studies (Good et al., 2011, Zhang et al., 2012). For pressure ejection experiments, signals were obtained every 60 s. After a stable baseline of 5 min, uptake inhibitors were applied for 12–15 min.

Detection of catecholamines from tissue homogenates. Sprague Dawley rats ($n = 6$) were anesthetized with isoflurane and decapitated. Brains were rapidly removed, placed in an ice-cooled 0.1 M percholoric acid solution, and coronally sectioned at ~1 mm thickness. LHb was bilaterally dissected over its anteroposterior length using hypodermic needles and scalpel blades. A portion of the medial habenula was included with LHb samples to detect DA, as described by Phillipson and Pycock (1982). Isolated tissue was pooled, briefly homogenized in 0.1 M perchloric acid for 10 s, and spun at 10,000 × *g* for 10 min in a centrifuge held at 4°C. The supernatant was separated into 20 μl aliquots and stored at −80C until further use. Protein concentrations were determined through the use of a bicinchoninic acid protein assay (Thermo Scientific). Concentrations of NE, 3,4-dihydroxyphenylacetic acid (DOPAC), and DA were analyzed using high performance liquid chromatography (HPLC) with electrochemical detection. Aliquots were injected into an Eicom HTEC-500 HPLC system with an integrated amperometric detector. Tissue homogenate samples (20 μl) were processed using a SC-30DS (ID 3.0 × 100 mm, 3 μm particulate silica) HPLC column and a precolumn (Eicom). The mobile phase consisted of 80% 0.1 M citrate-acetate buffer, pH 3.5, and 20% MeOH with 5 mg/L EDTA-2Na, 220 mg/L sodium octane sulfonate. Using a HTEC-500 pump with a flow rate of 400 μl/min and an applied potential of 750 mV versus Ag/AgCl, the resulting retention times for NE, DOPAC, and DA were as follows: 4.0–4.5, 6.0–6.5, and 8.5–9.0 min, respectively. Concentrations of monoamines were estimated using calibration curves obtained from external standards; NE #A7257, DOPAC #850217, and DA #H8502 were all purchased from Sigma-Aldrich. The final values were derived from total protein content determined by BCA and monoamine concentrations from HPLC analysis. A within-subjects ANOVA was used to examine overall differences in catecholamine content, and Sidak-adjusted pairwise comparisons were used to test specific differences.

Dopaminergic lesion. Thirty minutes before injection, Sprague Dawley rats ($n = 9$) were injected with the NE transport inhibitor desipramine (Sigma, 20 mg/kg, i.p.) to protect noradrenergic fibers. Rats were anesthetized with 1%–5% isofluorane and placed in a stereotaxic frame. A calibrated glass micropipette was filled with 6-hydroxydopamine (Sigma, 6-OHDA, 3 μg/μl in 0.1% ascorbic acid/0.9% saline) and directed toward VTA (−5.4 anteroposterior, −2.0 mediolateral at 10°, dorsoventral −8.2) (Mejías-Aponte et al., 2009). 6-OHDA was pressure-injected over 4 min (2 μl), and the micropipette was left in place an additional 15 min to limit diffusion up the pipette track. Three weeks following injection, LHb slices from these rats were obtained and used for whole-cell recordings. To verify 6-OHDA lesions, thick sections (280 μm) of LHb and VTA that were sectioned for whole-cell recordings were placed in 4% PFA for 1 week. Tissue was washed in PB and placed overnight in 0.3% Triton X-100 solution with anti-TH antibody (1:200; Millipore). Sections were then washed and either processed for fluorescence using fluorescein-conjugated donkey anti-mouse antibody (1:50; Jackson ImmunoResearch Laboratories; 2 h) or for DAB staining. For DAB staining, sections were incubated in biotinylated goat anti-mouse antibody (1:200; Vector Laboratories; 2 h), washed, incubated for 1 h in avidin-biotinylated HRP (1:200, ABC kit; Vector Laboratories), washed, and the peroxidase reaction was developed with 0.05% DAB and 0.03% H_2O_2.

Noradrenergic lesion. Sprague Dawley rats ($n = 10$) were anesthetized with 1%–5% isofluorane and placed in a stereotaxic frame. A calibrated glass micropipette was filled with *N*-(2-chloroethyl)-*N*-ethyl-2-bromobenzylamine (Sigma, DSP-4, 83–166 μg/μl), a selective noradrenergic neurotoxin (Szot et al., 2010), and directed toward the lateral ventricle (−0.8 anteroposterior, 1.4 mediolateral, −4.0 dorsoventral). DSP-4 was pressure-injected over 5 min (5 μl), and the micropipette was left in place for an additional 15 min to limit diffusion up the pipette track. DSP-4 was made fresh for each rat, the dosing of which was based on the results of Daw et al. (1985), and injected within 5 min of dilution. Three weeks following injection, rats were killed for whole-cell recordings.

Statistical analyses. Data are presented as mean ± SEM. Statistical comparisons were performed using either *t* tests or repeated-measures ANOVA using Prism (version 6.0, GraphPad Scientific), with significance assigned at $p \leq 0.05$.

Results

To examine the phenotype of the mesohabenular TH neurons, FluoroGold was iontophoresed in the rat LHb (Fig. 1*A*,*B*). Retrogradely labeled mesohabenular neurons were observed within the anteromedial VTA (Fig. 1*D*), typically medial to, and surrounding the fasciculus retroflexus, and anterior to the interpeduncular nucleus. Within the retrogradely labeled mesohabenular neurons, more than one-third of them (38.67 ± 2.84%) contained TH-protein detectable by immunofluorescence. Consistent with prior reports (Skagerberg et al., 1984; Gruber et al., 2007), more medial LHb injections tended to label mesohabenular TH neurons ventrally within the interfascicular and medial paranigral subregions whereas more lateral LHb injections tended to label mesohabenular TH neurons more dorsally across all subregions (Table 1). Because the vast majority of rat TH-expressing neurons located in the anteromedial VTA lack VMAT2 mRNA (Li et al., 2013), we determined, by *in situ* hybridization, whether mesohabenular TH neurons expressed VMAT2 mRNA. We found that most mesohabenular TH neurons did not express VMAT2 mRNA (96.1 ± 0.97%; 264 of 275 TH-expressing mesohabenular neurons) (Fig. 1*C*–*G*). These mesohabenular TH neurons lacking VMAT2 mRNA had low levels of TH immunofluorescence, likely reflecting the low copy numbers of TH mRNA, which characterizes TH-expressing neurons that lack detectable levels of VMAT2 mRNA (Li et al., 2013). The small population of mesohabenular TH neurons coexpressing VMAT2 mRNA did not exhibit a specific subregional localization (Table 1), but 8 of 11 neurons were observed caudally at the level of the interpeduncular nucleus.

We next determined the extent to which mesohabenular TH axons coexpressed VMAT2 within the LHb. To tag mesohabenular fibers, rats were injected in the VTA with a viral vector-expressing channelrhodopsin2 tethered to mCherry under the regulation of calcium/calmodulin protein kinase IIα promoter (AAV5-CaMKIIα-ChR2-mCherry). By confocal fluorescent microscopy, we observed within the LHb several mCherry-labeled

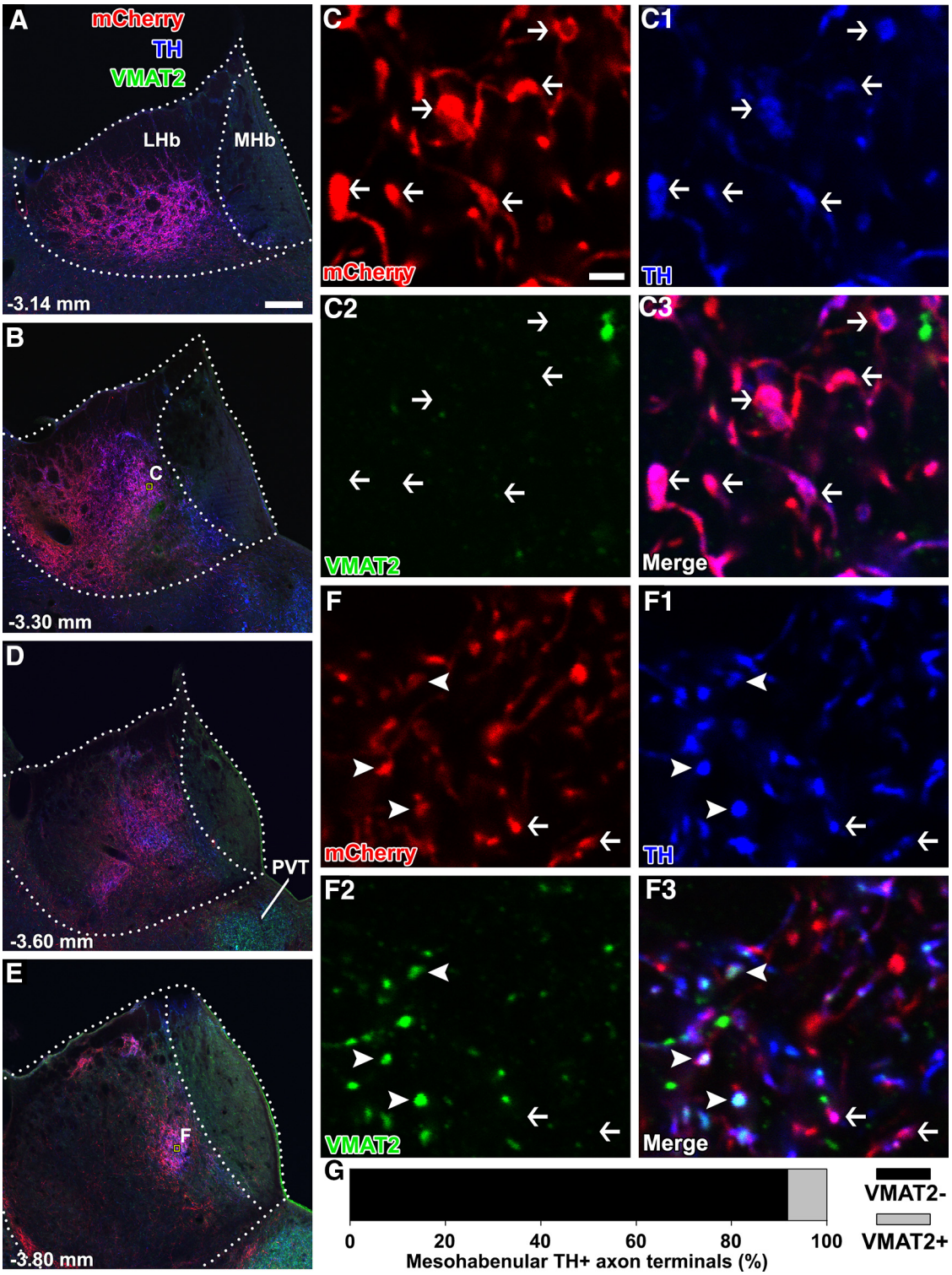

Figure 2. Most TH mesohabenular axons lack VMAT2. ***A***, ***B***, ***D***, ***E***, Triple immunofluorescence of coronal sections for detection of mCherry (red), TH (blue), and VMAT2 (green) at four anteroposterior levels of the habenula. VTA fibers expressing mCherry are present in the LHb, but not in the medial habenula (MHb). ***C***, Higher-magnification of boxed area in ***B***; fibers (arrows) expressing mCherry (***C***) and TH (***C1***) but lacking VMAT2 (***C2***), merge (***C3***). ***F***, Higher magnification of boxed area in ***E***; in addition to mCherry fibers containing TH (arrows), there is a subset of mCherry fibers (arrowheads) that contains both TH (***F1***) and VMAT2 (***F2***), merge (***F3***). Anteroposterior levels of the LHb (bregma, mm): ***A***, −3.14; ***B***, −3.30; ***C***, −3.60; ***D***, −3.80. Scale bars: ***A*** (applies to ***A***, ***B***, ***D***, ***E***), 100 μm; ***C*** (applies to ***C–C3***, ***F–F3***), 1 μm. ***G***, Mean percentage of mesohabenular TH-immunoreactive axons expressing or lacking VMAT2 mRNA (3392 VMAT2- from a total of 3737 mCherry-labeled TH-IR axons; mean ± SEM: VMAT2- 91.74 ± 1.89%; VMAT2 + 8.26 ± 1.89%). TH-IR and VMAT-IR appear to be highly co-localized outside LHb, with paraventricular thalamus (PVT).

fibers that contained TH. These mCherry-TH fibers were found from the rostral to the caudal aspects of the LHb and were more frequent in the medial LHb, where we focused our analysis (Fig. 2*A–E*). The majority of mCherry-TH fibers lacked VMAT2 signal (Fig. 2*C*,*G*). However, we consistently observed a few mCherry-TH fibers that coexpressed VMAT2 within a discrete region of the caudal LHb (Fig. 2*E*,*F*). These results confirm that the majority of VTA dopaminergic neurons that target LHb lack VMAT2.

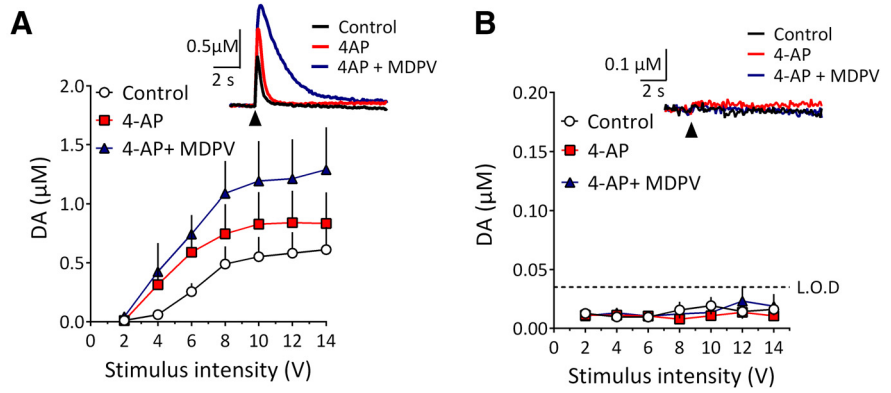

Figure 3. Absence of electrically evoked DA-like signals in the LHb. ***A***, Representative FSCV signals (top) in a NAc slice, demonstrating electrically evoked (1 ms pulse, arrow) DA release under control conditions, and its enhancement by both 4-AP (100 μM) and the uptake blocker MDPV (300 nM). Bottom, Averaged input–output curves examining FSCV signals at different electrical stimulus intensities in the NAc ($n = 5$ slices from 3 rats), in the absence and presence of 4-AP and MDPV. ***B***, Representative FSCV currents and averaged input–output curves in the LHb (7 slices, 4 rats). Neither 4-AP nor MDPV enhanced the signal, which did not rise above the calculated detection limit (dashed line). Error bars are SEM.

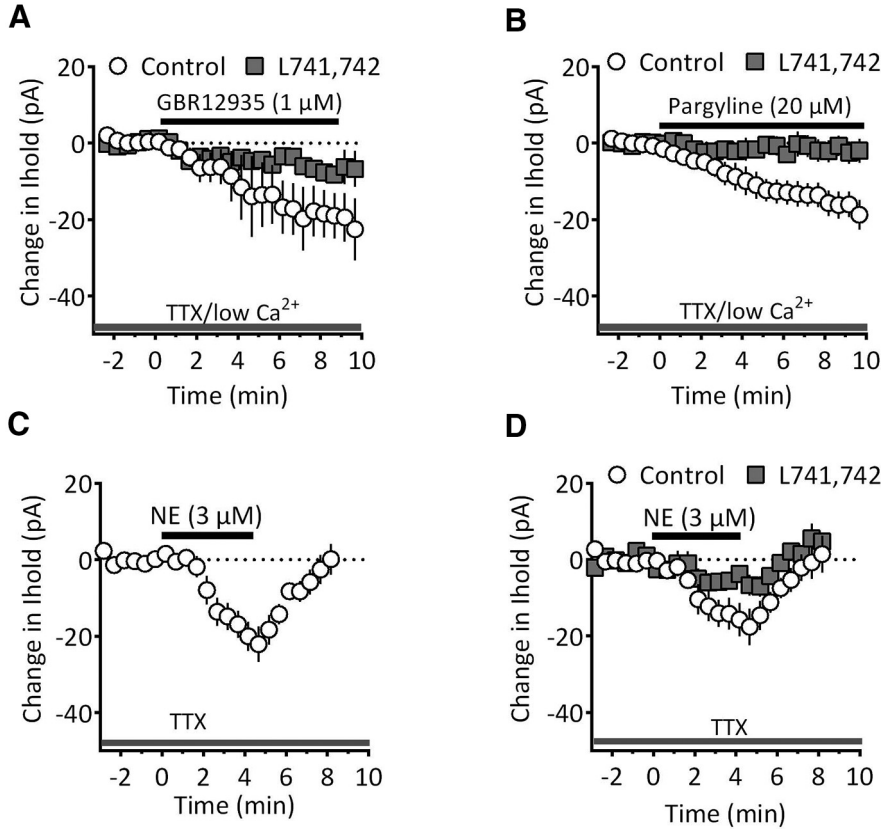

Figure 4. Dopamine D_4 receptor-mediated inward ion channel currents initiated by GBR12935, pargyline, or NE in LHb brain slices. ***A***, Mean ($n = 6$ neurons) time course of inward currents generated by the selective DAT inhibitor GBR12935 (1 μM) in LHb neurons maintained in low Ca^{2+} (0.3 mM) and TTX (200 nM). The effects of GBR12935 were significantly blocked by the selective D_4 antagonist L741,742 (200 nM; $n = 7$ neurons; two-way repeated-measures ANOVA, time × treatment, $F_{(1,24)} = 2.301$, $p < 0.001$). ***B***, Inward currents produced by the monoamine oxidase-B inhibitor pargyline (20 μM) in LHb slices maintained in low Ca^{2+} and TTX ($n = 6$ neurons). The effects of pargyline were significantly reduced by L741,742, indicating that dopamine D_4 receptors were activated ($n = 6$; two-way repeated-measures ANOVA, time × treatment, $F_{(1,25)} = 6.504$, $p < 0.001$). ***C***, Bath application of NE (3 μM) produced inward currents ($n = 6$ neurons) in the presence of TTX. ***D***, NE-induced inward currents were blocked by the DA-D_4 antagonist, L741,742 (200 nM). In these experiments ($n = 4$ neurons), NE was first applied and then washed. The D_4 antagonist was then applied for 10–15 min before a second application of NE. Currents were significantly attenuated following D_4 antagonist application (two-way repeated-measures ANOVA, time × treatment, $F_{(1,22)} = 2.586$, $p = 0.002$). Error bars are SEM.

Furthermore, we found that the minority of TH mesohabenular neurons that expressed VMAT2 targeted a discrete area of the caudal LHb, which appears to be a specific portion of the parvocellular subnucleus of the medial division of the LHb (Geisler et al., 2003).

We previously found that all rat TH-expressing VTA neurons coexpress L-aromatic amino decarboxylase mRNA (Li et al., 2013). This suggests that mesohabenular TH neurons can synthesize DA. However, the current data suggest that most of these neurons lack VMAT2 and thus lack the capacity for vesicular storage and conventional exocytotic release of DA. To investigate this, we used FSCV in brain slices containing either the LHb or nucleus accumbens (NAc). In the NAc, single-pulse local electrical stimulation evoked robust DA-like signals whose amplitude depended on stimulus intensity. Furthermore, these signals were increased when presynaptic action potentials were prolonged by the A-type K^+ channel blocker (4-aminopyridine, 4-AP, 100 μM), or when the DA uptake inhibitor, methylenedioxypyrovalerone (MDPV, 300 nM) (Baumann et al., 2013), was applied (Fig. 3*A*). In contrast, FSCV signals were never observed across a wide range of electrical stimulus intensities in rat LHb slices, and 4-AP or MDPV did not aid in their detection (Fig. 3*B*). In a few experiments, trains of pulses (25 Hz, 10 pulses) were also used. Although these trains also reliably elicited DA release in the NAc, they did not elicit responses in the LHb.

Prior studies in our laboratory demonstrated that the DA transport (DAT) inhibitors cocaine or GBR12935 generated ion channel currents in voltage-clamped rat LHb neurons via the activation of DA-D_4 receptors (Good et al., 2013; Jhou et al., 2013). However, the lack of VMAT2 in LHb-projecting VTA neurons and the absence of electrically evoked catecholamine signals suggest that the activation of DA receptors on LHb neurons during blockade of uptake may occur independently of vesicular release. To directly test this, we inhibited DA uptake or degradation during measurement of membrane currents in LHb neurons under conditions where neurotransmitter exocytosis was greatly limited by low extracellular Ca^{2+} (0.3 mM) and sodium channel blockade by tetrodotoxin (TTX, 200 nM). Using FSCV, we first confirmed that these conditions blocked electrically evoked, impulse-dependent DA release in the NAc (data not shown). Then we examined whether electrophysiological responses

reflecting the activation of postsynaptic DA-D_4 receptors were observed in the LHb. We found that, under these conditions, inward currents were observed upon application of GBR12935 (1 μM) (Fig. 4*A*). Similarly, when DA degradation was inhibited by the monoamine oxidase B (MAO-B) blocker, pargyline (20 μM), DA-D_4 receptor-mediated responses were observed in most LHb neurons (Fig. 4*B*).

The activation of DA-D_4 receptors during GBR12935 application, in the absence of impulse-dependent vesicle exocytosis, might indicate that DA is released from a nonvesicular pool in the LHb, whose extracellular levels are regulated by uptake and degradation. However, noradrenergic fibers are also located in the LHb (Gottesfeld, 1983), where tissue levels of NE exceed those of DA (Versteeg et al., 1976; Phillipson and Pycock, 1982). Moreover, NE has high affinity for DA-D_4 receptors (Newman-Tancredi et al., 1997; Cummings et al., 2010). Using HPLC, we confirmed that NE concentrations significantly exceeded those of DA and DOPAC in habenular homogenates ($F_{(2,10)} = 26.4$, $p < 0.001$; all Sidak-adjusted pairwise comparisons of NE vs DA and NE vs DOPAC, $p < 0.01$; mean ± SEM ng/mg protein: NE 520.77 ± 91.02; DA 118.69 ± 67.69; DOPAC 35.26 ± 14.84). Therefore, because NE and DA are present in the LHb, we next investigated the possible participation of NE in mediating the activation of DA-D_4 receptors in the LHb.

We first determined the effects of exogenous NE on the activation of DA-D_4 receptors on LHb neurons. We found that NE (3 μM) produced inward currents in LHb neurons that were blocked by the DA-D_4 receptor antagonist L741,742 (200 nM; Fig. 4*C*,*D*). We then examined the effects of GBR12935 on LHb neurons, following lesions of either DAergic or noradrenergic pathways under conditions where impulse-dependent neurotransmitter release was blocked (0.3 mM Ca^{2+}, 200 nM TTX). In contrast to LHb neurons obtained from control rats, inward currents were not observed upon GBR12935 application in cells obtained from rats treated with the noradrenergic pathway specific toxin, DSP-4 (Fig. 5*A*; 7 neurons, 3 rats). However, DA-D_4 receptor-mediated currents were still observed during GBR12935 application in LHb neurons obtained from rats that received intra-VTA injections of 6-hydroxydopamine, combined with systemic desipramine to protect noradrenergic fibers (Fig. 5*A*; 6 neurons, 3 rats).

These data suggest that DAT inhibition by GBR12935 can activate DA-D_4 receptors via extracellular accumulation of NE in LHb. However, it is also possible that GBR12935 acts on the NE transporter (NET) resulting in the elevation of extracellular NE that may then activate DA-D_4 receptors. To examine this possibility, we first determined the effects of the selective NET inhibitor nisoxetine (500 nM) (Tejani-Butt et al., 1990) on the LHb electrophysiological responses. We found that nisoxetine produced inward currents in LHb neurons that were significantly smaller than those generated by GBR12935 (nisoxetine, −9.8 ± 3.4 pA; GBR12935, −33 ± 9.5 pA, $p = 0.0189$, $t = 2.751$, df = 11, two tailed unpaired t test). Moreover, the nisoxetine-induced currents were not present in LHb neurons obtained from DSP-4 lesioned animals ($n = 9$ neurons, 4 rats; Fig. 5*B*), suggesting that, whereas the NET may be involved in NE clearance in the LHb, the majority of NE uptake occurs via the DAT. To examine this, we measured currents generated by pressure-application of NE in the LHb using FSCV and determined the effects of nisoxetine or GBR12935 on these responses (Fig. 6). We found that electrochemical NE signals were significantly increased by GBR12935 (1 μM; Fig. 6*C*, $n = 6$, $p = 0.0161$, two-tailed paired t test), but not by nisoxetine (500 nM; Fig. 6*D*, $n = 6$, $p = 0.1431$, two-tailed paired t test). Therefore, these results suggest that DAT predominantly mediates NE uptake in the rat LHb.

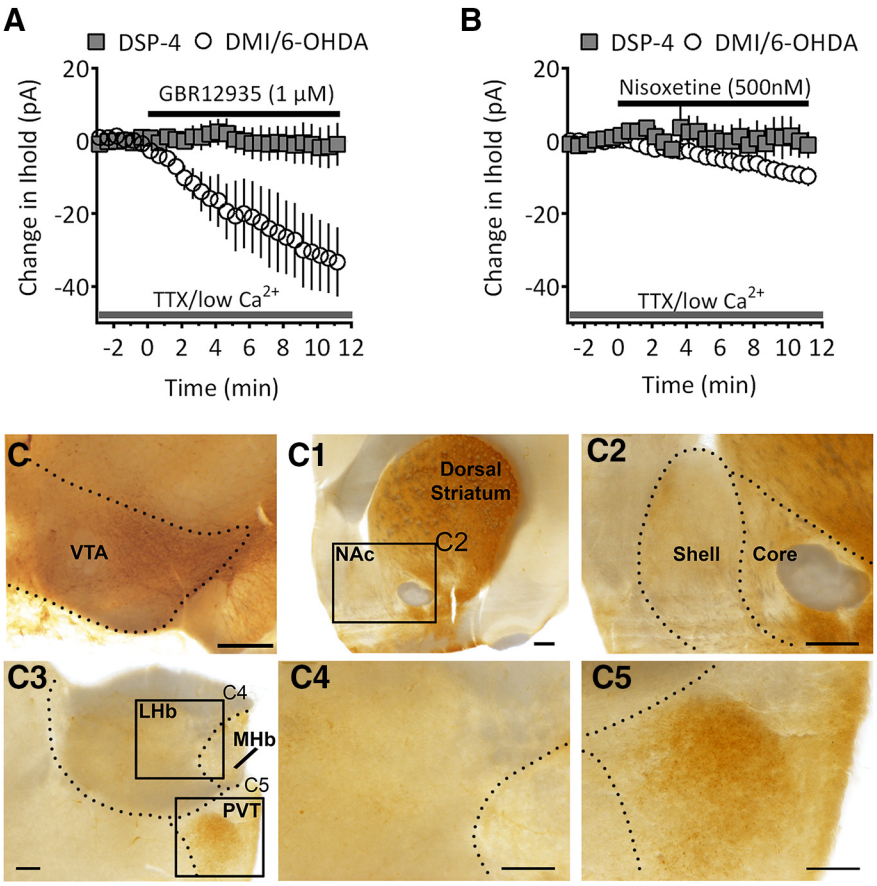

Figure 5. NE inputs, not VTA DA inputs to LHb, control inward currents elicited by GBR12935. ***A***, Inward currents produced by GBR12935 in LHb neurons recorded in slices are eliminated following intracranial DSP-4 ($n = 7$ neurons, 3 rats), but not following intra-VTA 6-OHDA in desipramine-pretreated rats ($n = 6$ neurons, 3 rats; two-way repeated-measures ANOVA, time × treatment, $F_{(1,28)} = 6.118$, $p < 0.001$). ***B***, Effects of the selective NET inhibitor nisoxetine (500 nM) in desipramine-pretreated, 6-OHDA-lesioned rats and following DSP4 lesions. Nisoxetine produced only a small inward current in LHb neurons recorded in slices from 6-OHDA-lesioned rats ($n = 11$ neurons, 4 rats) that was absent in slices from DSP4-lesioned rats ($n = 9$ neurons, 4 rats; two-way repeated-measures ANOVA, time × treatment, $F_{(1,28)} = 1.781$, $p = 0.009$). ***C***, Loss of TH-IR cell bodies in the VTA (***C***) and fibers following 6-OHDA lesion of the VTA. TH-IR fibers were not detected in the nucleus accumbens shell (***C1***, ***C2***) or LHb (***C3***, ***C4***), but were found within the paraventricular thalamus (PVT; ***C5***). Scale bars: ***C–C5***, 0.5 μm. Error bars are SEM.

Discussion

The present study demonstrates that the recently discovered VTA TH-expressing neurons that lack VMAT2 mRNA project to LHb. We show that these mesohabenular neurons are incapable of releasing DA via canonical neurotransmitter exocytosis because

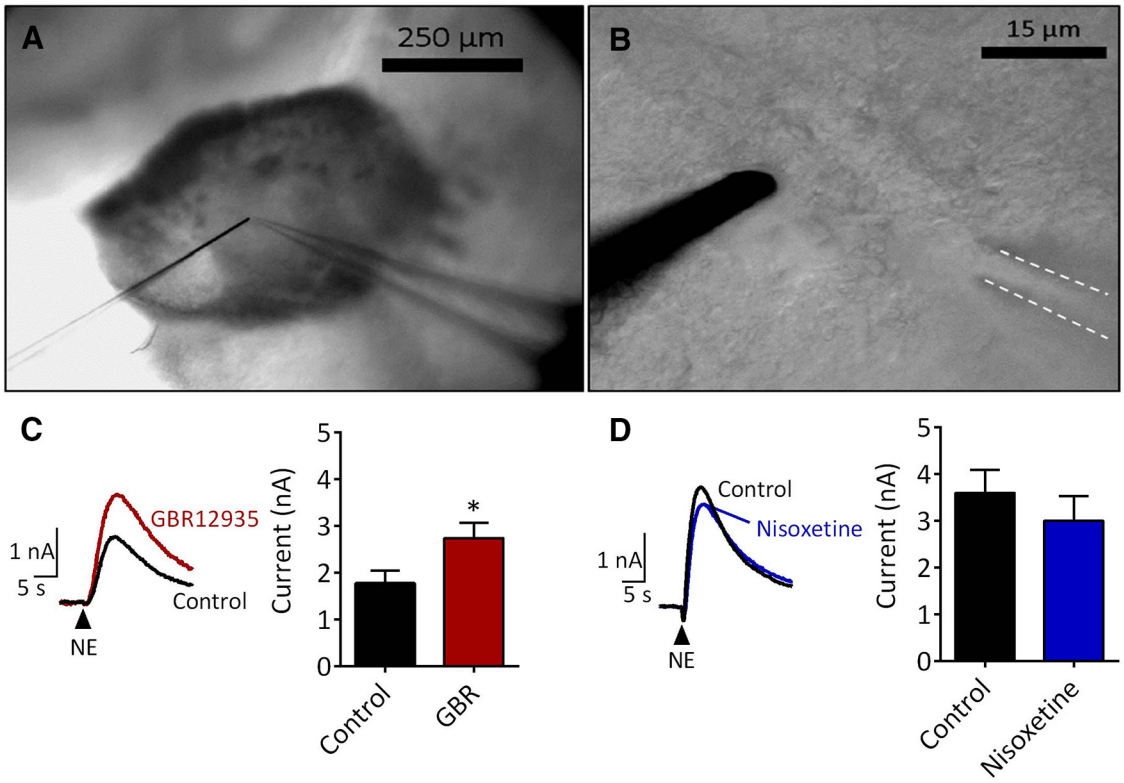

Figure 6. Clearance of exogenous NE in the LHb is inhibited by the selective DAT inhibitor GBR12935 and not by the selective NET inhibitor nisoxetine. ***A***, Low-power image of a slice containing the LHb. A carbon fiber electrode (left) was used to detect NE (10 μM) applied via pressure ejection from the pipette seen at right. ***B***, Higher-magnification image of the carbon fiber electrode. The pressure-ejection pipette was positioned just above and to the right of the carbon fiber, outside the optical plane of focus (dashed lines). ***C***, Left, Representative signals (average of 4 responses, every 60 s) taken before (control) and during bath application of GBR12935 (1 μM). Right, Signals were significantly potentiated ($n = 6$ slices) by GBR12935. *$p = 0.0161$ (two-tailed paired *t* test). ***D***, Signals obtained before and during application of nisoxetine (500 nM). The effect of nisoxetine was not significant ($n = 6$ slices). $p = 0.1431$ (two-tailed paired *t* test). Error bars are SEM.

they lack VMAT2 and therefore cannot package DA into synaptic vesicles. We also found that elevation of extracellular catecholamine levels through inhibition of either the DAT, or MAO under conditions where impulse-dependent release is blocked, results in the activation of DA-D_4 receptors on LHb neurons and that this depends upon intact noradrenergic fibers. Collectively, these data suggest that, whereas vesicular DA release by mesohabenular inputs is limited by the absence of VMAT2, impulse-independent NE release can still activate postsynaptic DA receptors in the rat LHb, and this is under the regulation of uptake and enzymatic degradation.

We recently showed that in the rat there are at least eight classes of VTA neurons that project to the LHb (Root et al., 2014a). Among these, ~30% of mesohabenular neurons express TH immunoreactivity and coexpress different combinations of glutamatergic and GABAergic signaling markers (Root et al., 2014a). Here, we found that, despite the heterogeneity among these mesohabenular TH neurons, they predominantly share in common a lack of detectable expression of VMAT2 mRNA in their cells bodies, and a lack of detectable VMAT2 protein in most of their axons within the LHb. Thus, the presence of vesicles containing DA within the rat mesohabenular pathway, under normal conditions, is minimal. Consistent with the lack of a major pool of DA within synaptic vesicles in the LHb, local electrical stimulation did not result in detectable DA-like currents using FSCV. The absence of a major pool of vesicular DA from the VTA seems to be a general feature in rodents, as a recent optogenetic study of VTA dopaminergic efferents has also reported a lack of DA release in the mouse LHb (Stamatakis et al., 2013).

Despite the lack of detectable DA-like FSCV signals in the LHb, DA-D_4 receptors were activated following inhibition of DAT or MAO, and this was detected as an increase in whole-cell conductance and the generation of excitatory inward currents (Good et al., 2013). Given these results, it was reasonable to infer that the activation of D_4 receptors during DAT and MAO inhibition, and under conditions of limited vesicular exocytosis (i.e., low Ca^{2+} and TTX), resulted from an increase in extracellular levels of DA via a nonvesicular release process. However, the LHb also receives innervation from dopamine β-hydroxylase containing noradrenergic fibers, largely arising from the locus ceruleus (Phillipson and Pycock, 1982; Gottesfeld, 1983; Gruber et al., 2007). Because NE is a potent agonist at DA-D_4 receptors (Newman-Tancredi et al., 1997; Cummings et al., 2010), we hypothesized that NE is released in the LHb, and this is the primary catecholamine interacting with D_4 receptors, rather than DA. In support of this hypothesis, D_4 currents were activated by exogenously applied NE, and the ability of the DAT inhibitor GBR12935 to generate these currents was lost following selective lesions of noradrenergic fibers by DSP-4. These findings, together with the inability of 6-OHDA lesions of the VTA to disrupt the effects of GBR12935, suggest that it is NE, rather than DA, that activates DA-D_4 receptors on LHb neurons when uptake is blocked. These results do not, however, preclude the possibility that DA could be released from noradrenergic fibers, as demonstrated in other brain regions (Devoto et al., 2005; Smith and Greene, 2012). Because NE and DA are indistinguishable using FSCV (Michael and Wightman, 1999), the absence of detectable voltammetric signals using electrical stimulation, coupled with the

electrophysiological responses observed under conditions of limited exocytosis, suggests that NE release may occur via impulse-independent mechanisms in the CNS, as suggested previously (Chiti and Teschemacher, 2007).

The present data suggest that, despite the absence of vesicular DA release from TH-expressing VTA neurons projecting to the LHb, cocaine and other uptake inhibitors may influence LHb activity via NE. Although the relevance of this noradrenergic influence on LHb function and behavior is not yet clear, there is a growing body of evidence to suggest that the aversive properties of cocaine are dependent on catecholaminergic actions in the LHb (Dougherty et al., 1990; Wirtshafter et al., 1994; Jhou et al., 2009a, 2013; Zahm et al., 2010; Maroteaux and Mameli, 2012; Good et al., 2013; Zuo et al., 2013). Moreover, LHb circuit interactions with the VTA, RMTg, and dorsal raphe nucleus play significant roles in mediating the effects of psychostimulants, as well as aversive events (Paris and Cunningham, 1994; Wirtshafter et al., 1994; Matsumoto and Hikosaka, 2007, 2009; Jhou et al., 2009a,b, 2013; Friedman et al., 2010; Zahm et al., 2010; Hong et al., 2011; Lammel et al., 2012; Lavezzi et al., 2012; Stamatakis and Stuber, 2012; Brown and Shepard, 2013; Nair et al., 2013; Root et al., 2014b). As the noradrenergic pathway originating in the locus ceruleus, a well-established mediator of stress and aversion (Delfs et al., 2000; Aston-Jones and Kalivas, 2008), we hypothesize that the actions of NE may contribute to the processing of aversive events and anti-reward processes in the LHb.

In conclusion, we found that the rat VTA TH neurons innervating the LHb in their vast majority lack VMAT2 mRNA, and that the majority of TH axons from these mesohabenular neurons also lack VMAT2 protein. Thus, we inferred that within the mesohabenular pathway, under normal conditions, DA accumulation in synaptic vesicles is minimal or absent. Consistent with this finding, DA was not detected by FSCV following local electrical stimulation within the LHb. Our findings also reveal a surprising contribution of NE in the regulation of D_4-receptor-mediated LHb inward currents. Thus, we conclude that within the LHb, D_4-receptor activation is primarily mediated by NE, rather than DA.

References

Aston-Jones G, Kalivas PW (2008) Brain norepinephrine rediscovered in addiction research. Biol Psychiatry 63:1005–1006. CrossRef Medline

Balcita-Pedicino JJ, Omelchenko N, Bell R, Sesack SR (2011) The inhibitory influence of the lateral habenula on midbrain dopamine cells: ultrastructural evidence for indirect mediation via the rostromedial mesopontine tegmental nucleus. J Comp Neurol 519:1143–1164. CrossRef Medline

Baumann MH, Partilla JS, Lehner KR, Thorndike EB, Hoffman AF, Holy M, Rothman RB, Goldberg SR, Lupica CR, Sitte HH, Brandt SD, Tella SR, Cozzi NV, Schindler CW (2013) Powerful cocaine-like actions of 3,4-methylenedioxypyrovalerone (MDPV), a principal constituent of psychoactive 'bath salts' products. Neuropsychopharmacology 38:552–562. CrossRef Medline

Bromberg-Martin ES, Hikosaka O (2011) Lateral habenula neurons signal errors in the prediction of reward information. Nat Neurosci 14:1209–1216. CrossRef Medline

Brown PL, Shepard PD (2013) Lesions of the fasciculus retroflexus alter footshock-induced cFos expression in the mesopontine rostromedial tegmental area of rats. PLoS One 8:e60678. CrossRef Medline

Chiti Z, Teschemacher AG (2007) Exocytosis of norepinephrine at axon varicosities and neuronal cell bodies in the rat brain. FASEB J 21:2540–2550. CrossRef Medline

Christoph GR, Leonzio RJ, Wilcox KS (1986) Stimulation of the lateral habenula inhibits dopamine-containing neurons in the substantia nigra and ventral tegmental area of the rat. J Neurosci 6:613–619. Medline

Cummings DF, Ericksen SS, Goetz A, Schetz JA (2010) Transmembrane segment five serines of the D4 dopamine receptor uniquely influence the interactions of dopamine, norepinephrine, and Ro10-4548. J Pharmacol Exp Ther 333:682–695. CrossRef Medline

Daw NW, Videen TO, Parkinson D, Rader RK (1985) DSP-4 (N-(2-chloroethyl)-*N*-ethyl-2-bromobenzylamine) depletes noradrenaline in kitten visual cortex without altering the effects of monocular deprivation. J Neurosci 5:1925–1933. Medline

Delfs JM, Zhu Y, Druhan JP, Aston-Jones G (2000) Noradrenaline in the ventral forebrain is critical for opiate withdrawal-induced aversion. Nature 403:430–434. CrossRef Medline

Devoto P, Flore G, Saba P, Fà M, Gessa GL (2005) Stimulation of the locus coeruleus elicits noradrenaline and dopamine release in the medial prefrontal and parietal cortex. J Neurochem 92:368–374. CrossRef Medline

Dougherty PM, Qiao JT, Wiggins RC, Dafny N (1990) Microiontophoresis of cocaine, desipramine, sulpiride, methysergide, and naloxone in habenula and parafasciculus. Exp Neurol 108:241–246. CrossRef Medline

Friedman A, Lax E, Dikshtein Y, Abraham L, Flaumenhaft Y, Sudai E, Ben-Tzion M, Ami-Ad L, Yaka R, Yadid G (2010) Electrical stimulation of the lateral habenula produces enduring inhibitory effect on cocaine seeking behavior. Neuropharmacology 59:452–459. CrossRef Medline

Geisler S, Andres KH, Veh RW (2003) Morphologic and cytochem criteria for the identification and delineation of individual subnuclei within the lateral habenular complex of the rat. J Comp Neurol 458:78–97. CrossRef Medline

Good CH, Hoffman AF, Hoffer BJ, Chefer VI, Shippenberg TS, Bäckman CM, Larsson NG, Olson L, Gellhaar S, Galter D, Lupica CR (2011) Impaired nigrostriatal function precedes behavioral deficits in a genetic mitochondrial model of Parkinson's disease. FASEB J 25:1333–1344. CrossRef Medline

Good CH, Wang H, Chen YH, Mejias-Aponte CA, Hoffman AF, Lupica CR (2013) Dopamine D4 receptor excitation of lateral habenula neurons via multiple cellular mechanisms. J Neurosci 33:16853–16864. CrossRef Medline

Gottesfeld Z (1983) Origin and distribution of noradrenergic innervation in the habenula: a neurochemical study. Brain Res 275:299–304. CrossRef Medline

Gruber C, Kahl A, Lebenheim L, Kowski A, Dittgen A, Veh RW (2007) Dopaminergic projections from the VTA substantially contribute to the mesohabenular pathway in the rat. Neurosci Lett 427:165–170. CrossRef Medline

Guillot TS, Miller GW (2009) Protective actions of the vesicular monoamine transporter 2 (VMAT2) in monoaminergic neurons. Mol Neurobiol 39:149–170. CrossRef Medline

Hong S, Jhou TC, Smith M, Saleem KS, Hikosaka O (2011) Negative reward signals from the lateral habenula to dopamine neurons are mediated by rostromedial tegmental nucleus in primates. J Neurosci 31:11457–11471. CrossRef Medline

Jhou TC, Fields HL, Baxter MG, Saper CB, Holland PC (2009a) The rostromedial tegmental nucleus (RMTg), a GABAergic afferent to midbrain dopamine neurons, encodes aversive stimuli and inhibits motor responses. Neuron 61:786–800. CrossRef Medline

Jhou TC, Geisler S, Marinelli M, Degarmo BA, Zahm DS (2009b) The mesopontine rostromedial tegmental nucleus: a structure targeted by the lateral habenula that projects to the ventral tegmental area of Tsai and substantia nigra compacta. J Comp Neurol 513:566–596. CrossRef Medline

Jhou TC, Good CH, Rowley CS, Xu SP, Wang H, Burnham NW, Hoffman AF, Lupica CR, Ikemoto S (2013) Cocaine drives aversive conditioning via delayed activation of dopamine-responsive habenular and midbrain pathways. J Neurosci 33:7501–7512. CrossRef Medline

Ji H, Shepard PD (2007) Lateral habenula stimulation inhibits rat midbrain dopamine neurons through a GABA(A) receptor-mediated mechanism. J Neurosci 27:6923–6930. CrossRef Medline

Lammel S, Lim BK, Ran C, Huang KW, Betley MJ, Tye KM, Deisseroth K, Malenka RC (2012) Input-specific control of reward and aversion in the ventral tegmental area. Nature 491:212–217. CrossRef Medline

Lavezzi HN, Parsley KP, Zahm DS (2012) Mesopontine rostromedial tegmental nucleus neurons projecting to the dorsal raphe and pedunculopontine tegmental nucleus: psychostimulant-elicited Fos expression and collateralization. Brain Struct Funct 217:719–734. CrossRef Medline

Li B, Piriz J, Mirrione M, Chung C, Proulx CD, Schulz D, Henn F, Malinow R (2011) Synaptic potentiation onto habenula neurons in the learned helplessness model of depression. Nature 470:535–539. CrossRef Medline

Li X, Qi J, Yamaguchi T, Wang HL, Morales M (2013) Heterogeneous composition of dopamine neurons of the rat A10 region: molecular evidence for diverse signaling properties. Brain Struct Funct 218:1159–1176. CrossRef Medline

Maroteaux M, Mameli M (2012) Cocaine evokes projection-specific synaptic plasticity of lateral habenula neurons. J Neurosci 32:12641–12646. CrossRef Medline

Matsumoto M, Hikosaka O (2007) Lateral habenula as a source of negative reward signals in dopamine neurons. Nature 447:1111–1115. CrossRef Medline

Matsumoto M, Hikosaka O (2009) Representation of negative motivational value in the primate lateral habenula. Nat Neurosci 12:77–84. CrossRef Medline

Mejías-Aponte CA, Drouin C, Astor-Jones G (2009) Adrenergic and noradrenergic innervation of the midbrain ventral tegmental area and retrorubral field: prominent inputs from medullary homeostatic centers. J Neurosci 29:3613–3626. CrossRef Medline

Michael DJ, Wightman RM (1999) Electrochemical monitoring of biogenic amine neurotransmission in real time. J Pharm Biomed Anal 19:33–46. CrossRef Medline

Nair SG, Strand NS, Neumaier JF (2013) DREADDing the lateral habenula: a review of methodological approaches for studying lateral habenula function. Brain Res 1511:93–101. CrossRef Medline

Newman-Tancredi A, Audinot-Bouchez V, Gobert A, Millan MJ (1997) Noradrenaline and adrenaline are high affinity agonists at dopamine D4 receptors. Eur J Pharmacol 319:379–383. CrossRef Medline

Omelchenko N, Bell R, Sesack SR (2009) Lateral habenula projections to dopamine and GABA neurons in the rat ventral tegmental area. Eur J Neurosci 30:1239–1250. CrossRef Medline

Paris JM, Cunningham KA (1994) Habenula lesions decrease the responsiveness of dorsal raphe serotonin neurons to cocaine. Pharmacol Biochem Behav 49:555–560. CrossRef Medline

Paxinos G, Watson C (2007) The rat brain in stereotaxic coordinates. Sydney, Australia: Academic.

Phillipson OT, Griffith AC (1980) The neurones of origin for the mesohabenular dopamine pathway. Brain Res 197:213–218. CrossRef Medline

Phillipson OT, Pycock CJ (1982) Dopamine neurons of the ventral tegmentum project to both medial and lateral habenula: some implications for Habenular function. Exp Brain Res 45:89–94. CrossRef Medline

Root DH, Mejias-Aponte CA, Zhang S, Wang HL, Hoffman AF, Lupica CR, Morales M (2014a) Single rodent mesohabenular axons release glutamate and GABA. Nat Neurosci 17:1543–1551. CrossRef Medline

Root DH, Mejias-Aponte CA, Qi J, Morales M (2014b) Role of glutamatergic projections from ventral tegmental area to lateral habenula in aversive conditioning. J Neurosci 34:13906–13910. CrossRef Medline

Skagerberg G, Lindvall O, Björklund A (1984) Origin, course and termination of the mesohabenular dopamine pathway in the rat. Brain Res 307:99–108. CrossRef Medline

Smith CC, Greene RW (2012) CNS dopamine transmission mediated by noradrenergic innervation. J Neurosci 32:6072–6080. CrossRef Medline

Stamatakis AM, Stuber GD (2012) Activation of lateral habenula inputs to the ventral midbrain promotes behavioral avoidance. Nat Neurosci 15:1105–1107. CrossRef Medline

Stamatakis AM, Jennings JH, Ung RL, Blair GA, Weinberg RJ, Neve RL, Boyce F, Mattis J, Ramakrishnan C, Deisseroth K, Stuber GD (2013) A unique population of ventral tegmental area neurons inhibits the lateral habenula to promote reward. Neuron 80:1039–1053. CrossRef Medline

Swanson LW (1982) The projections of the ventral tegmental area and adjacent regions: a combined fluorescent retrograde tracer and immunofluorescence study in the rat. Brain Res Bull 9:321–353. CrossRef Medline

Szot P, Miguelez C, White SS, Franklin A, Sikkema C, Wilkinson CW, Ugedo L, Raskind MA (2010) A comprehensive analysis of the effect of DSP4 on the locus coeruleus noradrenergic system in the rat. Neuroscience 166:279–291. CrossRef Medline

Tejani-Butt SM, Brunswick DJ, Frazer A (1990) [^{3}H]Nisoxetine: a new radioligand for norepinephrine uptake sites in brain. Eur J Pharmacol 191:239–243. CrossRef Medline

Versteeg DH, Van Der Gugten J, De Jong W, Palkovits M (1976) Regional concentrations of noradrenaline and dopamine in rat brain. Brain Res 113:563–574. CrossRef Medline

Wirtshafter D, Asin KE, Pitzer MR (1994) Dopamine agonists and stress produce different patterns of Fos-like immunoreactivity in the lateral habenula. Brain Res 633:21–26. CrossRef Medline

Wise RA, Rompre PP (1989) Brain dopamine and reward. Annu Rev Psychol 40:191–225. CrossRef Medline

Zahm DS, Becker ML, Freiman AJ, Strauch S, Degarmo B, Geisler S, Meredith GE, Marinelli M (2010) Fos after single and repeated self-administration of cocaine and saline in the rat: emphasis on the basal forebrain and recalibration of expression. Neuropsychopharmacology 35:445–463. CrossRef Medline

Zhang Y, Granholm AC, Huh K, Shan L, Diaz-Ruiz O, Malik N, Olson L, Hoffer BJ, Lupica CR, Hoffman AF, Bäckman CM (2012) PTEN deletion enhances survival, neurite outgrowth and function of dopamine neuron grafts to MitoPark mice. Brain 135:2736–2749. CrossRef Medline

Zuo W, Chen L, Wang L, Ye JH (2013) Cocaine facilitates glutamatergic transmission and activates lateral habenular neurons. Neuropharmacology 70:180–189. CrossRef Medline